Ho et al. *Zool. Res.* 2023, 44(3): 650−662
https://doi.org/10.24272/j.issn.2095-8137.2022.281

ZR | Zoological Research

Article Open Access

Decoding hereditary spastic paraplegia pathogenicity through transcriptomic profiling

Nicolas James Ho[1], Xiao Chen[2,3,4,5,6], Yong Lei[7,8,*], Shen Gu[1,9,10,11,*]

[1] *School of Biomedical Sciences*, *Faculty of Medicine*, *The Chinese University of Hong Kong*, *Hong Kong SAR*, *China*
[2] *Dr. Li Dak Sum-Yip Yio Chin Center for Stem Cells and Regenerative Medicine and Department of Orthopedic Surgery of the Second Affiliated Hospital*, *Zhejiang University School of Medicine*, *Hangzhou*, *Zhejiang* 310058, *China*
[3] *Key Laboratory of Tissue Engineering and Regenerative Medicine of Zhejiang Province*, *Zhejiang University School of Medicine*, *Hangzhou*, *Zhejiang* 310058, *China*
[4] *Zhejiang University-University of Edinburgh Institute* & *School of Basic Medicine*, *Zhejiang University School of Medicine*, *Hangzhou*, *Zhejiang* 310058, *China*
[5] *Department of Sports Medicine*, *Zhejiang University School of Medicine*, *Hangzhou*, *Zhejiang* 310058, *China*
[6] *China Orthopedic Regenerative Medicine Group (CORMed)*, *Hangzhou*, *Zhejiang*, 310058 *China*
[7] *School of Medicine*, *The Chinese University of Hong Kong (Shenzhen)*, *Shenzhen*, *Guangdong* 518172, *China*
[8] *The Chinese University of Hong Kong (Shenzhen)*, *Shenzhen Futian Biomedical Innovation R&D Center*, *Shenzhen*, *Guangdong 518172*, *China*
[9] *Key Laboratory for Regenerative Medicine*, *Ministry of Education*, *School of Biomedical Sciences*, *Faculty of Medicine*, *The Chinese University of Hong Kong*, *Hong Kong SAR*, *China*
[10] *Kunming Institute of Zoology - The Chinese University of Hong Kong (KIZ-CUHK) Joint Laboratory of Bioresources and Molecular Research of Common Diseases*, *Hong Kong SAR*, *China*
[11] *Hong Kong Branch of CAS Center for Excellence in Animal Evolution and Genetics*, *The Chinese University of Hong Kong*, *Hong Kong SAR*, *China*

ABSTRACT

Hereditary spastic paraplegia (HSP) is a group of genetic motor neuron diseases resulting from length-dependent axonal degeneration of the corticospinal upper motor neurons. Due to the advancement of next-generation sequencing, more than 70 novel HSP disease-causing genes have been identified in the past decade. Despite this, our understanding of HSP physiopathology and the development of efficient management and treatment strategies remain poor. One major challenge in studying HSP pathogenicity is selective neuronal vulnerability, characterized by the manifestation of clinical symptoms that are restricted to specific neuronal populations, despite the presence of germline disease-causing variants in every cell of the patient. Furthermore, disease genes may exhibit ubiquitous expression patterns and involve a myriad of different pathways to cause motor neuron degeneration. In the current review, we explore the correlation between transcriptomic data and clinical manifestations, as well as the importance of interspecies models by comparing tissue-specific transcriptomic profiles of humans and mice, expression patterns of different genes in the brain during development, and single-cell transcriptomic data from related tissues. Furthermore, we discuss the potential of emerging single-cell RNA sequencing technologies to resolve unanswered questions related to HSP pathogenicity.

Keywords: Hereditary spastic paraplegia; Motor neuron degeneration; Disease pathogenicity; Transcriptome analysis; Single-cell RNA sequencing

INTRODUCTION

Hereditary spastic paraplegia (HSP) refers to a group of

Received: 30 December 2022; Accepted: 10 May 2023; Online: 10 May 2023

Foundation items: This study was supported by the General Research Fund from the Research Grants Council of Hong Kong (24101921), Direct Grant from the Chinese University of Hong Kong (2020.096), National Natural Science Foundation of China (32170583, 82202045), Hong Kong RGC-CRF Equipment Fund C5033-19E, Shenzhen-Hong Kong Cooperation Zone for Technology and Innovation (HZQB-KCZYB-2020056), and Ganghong Young Scholar Development Fund (to Y.L.). Additional support was provided by the Hong Kong Branch of the CAS Center for Excellence in Animal Evolution and Genetics, Chinese University of Hong Kong (8601010)

*Corresponding authors, E-mail: leiyong@cuhk.edu.cn; shengu@cuhk.edu.hk

inheritable neurodegenerative diseases involving corticospinal motor neurons (CSMNs) in the corticospinal tract (CST) of the pyramidal tract. The CST constitutes part of the descending spinal tract that houses CSMN axons, along which movement-related signals propagate from the cerebral cortex to the spinal cord, and subsequently to effectors, such as muscles, to control limb movement. Degeneration of axons in the CST can lead to failure of the affected CSMNs to deliver movement-related signals to the corresponding downstream effectors. In the case of HSP, the long CSMN axons that affect the lower limbs are particularly prone to degeneration following length-dependent degradation (dying back), wherein the axons degenerate from the terminal and propagate retrogradely towards the cell body (Deluca et al., 2004). As a result, HSP patients are likely to suffer from progressive lower limb weakness and spasticity, with difficulty in walking.

Subtypes of HSP vary by age of onset, severity, and progression course. They can generally be divided into syndromic (“complicated” or “complex”) and non-syndromic (“uncomplicated” or “pure”) subtypes, depending on the presented symptoms. Symptoms of non-syndromic HSP subtypes are mostly limited to lower-limb weakness and spasticity, with possible sensory and bladder disturbances. Syndromic HSP subtypes are characterized by the impairments presented in non-syndromic HSP as well as complications in other systems and/or neurological findings (Hedera, 1993). In total, 71 subtypes of HSP have been documented in the spastic paraplegia phenotypic series (ID:PS303350) from the Online Mendelian Inheritance in Man (OMIM) database (2021) (last accessed on 14 September 2021). Nevertheless, it is estimated that approximately half of HSP cases have not been molecularly diagnosed (Ruano et al., 2014). Despite ongoing research, the disease-causing mechanisms underlying the defects of this group remain largely unknown, and patients are primarily managed by symptomatic treatment with no cure currently available (Bellofatto et al., 2019).

HSP has been reviewed from different perspectives, including historical (Walusinski, 2020), clinical and disease presentation (De Souza et al., 2017; Klebe et al., 2015), treatment and management (Bellofatto et al., 2019; Gumeni et al., 2021), and relevance of animal models (Genc et al., 2019). The emergence of next-generation sequencing (NGS) in research and clinical diagnosis, as well as transcriptomic analysis via NGS-based bulk RNA sequencing (RNA-seq) and single-cell RNA sequencing (scRNA-seq), has provided a wealth of information regarding expression profiles in various tissue and cell types. Here, we used data obtained from 16 975 protein-coding genes across 32 normal human tissues that were sequenced, mapped, and uploaded to an online platform as part of the Human Protein Atlas portal (Uhlen et al., 2015). The EMBL-EBI expression atlas portal was utilized to analyze available human and mouse expression datasets of the forebrain and hindbrain along a developmental timeline (Cardoso-Moreira et al., 2019). ScRNA-seq transcriptomic data from the human and mouse brain, documented on the Allen Institute website (Allen Institute, 2021) and Neuroscience Multi-Omic Analytics browser (Orvis et al., 2021), were also investigated. As HSP genes may also correlate with other neurological conditions, the potential implication of HSP genes in Alzheimer’s disease was investigated with reference to the AlzData database (last accessed on 24 November 2022) (Supplementary Tables S1, S2) (Xu et al., 2018).

This paper examines the relationship between transcriptomic profiles and clinical presentations in HSP, as well as species-specific transcriptomic profiles and interspecies differential phenotypic outcomes, with further exploration of the potential of NGS platforms to study diseases involving a minor population of cells. By analyzing cell-specific, tissue-specific, and time-specific gene expression profiles of HSP genes in humans and mice, this review should shed light on the pathogenicity of HSP genes and contribute to our understanding of upper motor neuron degenerative diseases and other neurological conditions.

MATERIALS AND METHODS

Correlation between HSP gene expression and clinical presentation

A list of genes associated with various HSP subtypes was obtained from the OMIM database (Supplementary Table S1, last accessed on 14 September 2021). Tissue RNA expression profiles of the HSP-associated genes were obtained from the v20 Human Protein Atlas portal in normalized expression (NX) (last accessed on 14 November 2021). In brief, previous studies summarized and aggregated raw counts of mapped reads over each gene to calculate transcripts per million (TPM) based on quality-filtered reads from RNA-seq data. (Robinson & Oshlack, 2010, Van Den Berg et al., 2006). Except for expression levels in blood, all normalized datasets were subsequently combined using batch correction with the “removeBatchEffect” function in the R package Limma (Uhlen et al., 2015). Normalized datasets marked NX were then retrieved for further analysis. The tissue expression profiles were tabulated and grouped based on the earliest reported onset age in their corresponding HSP subtype patients. For better visualization, the expression in each tissue class was subsequently averaged and shaded (Figure 1). Metadata, such as syndromic or non-syndromic subtypes, earliest reported age of onset, and autosomal dominant (AD), autosomal recessive (AR), or X-linked recessive (XLR) modes of inheritance, were also labeled based on previous literature and database searches (Bellofatto et al., 2019; De Souza et al., 2017; Online Mendelian Inheritance in Man, 2021; Orphanet Rare Disease Portal, 2021). Literature search on disease mechanisms of AD-HSP was performed, and pLI scores of genes associated with AD-HSP were obtained from the gnomAD browser (Karczewski et al., 2020) (last accessed on 20 May 2022).

Interspecies relevance of HSP gene expression profiles

Data on HSP gene expression with respect to developmental stages were retrieved from the EMBL-EBI expression atlas portal in TPM (Cardoso-Moreira et al., 2019) (last accessed on 11 December 2021). Pre- and postnatal expression levels of HSP genes in the forebrain and hindbrain of both humans and mice were tabulated (Supplementary Figure S1). The relative fold-change in expression was calculated with reference to the earliest time point with detectable expression along either the prenatal and/or postnatal developmental timeline (Figure 2). In general, expression at 4 weeks post conception (wpc), the earliest available time point, was defined as the reference level for calculating relative fold-change in the prenatal human

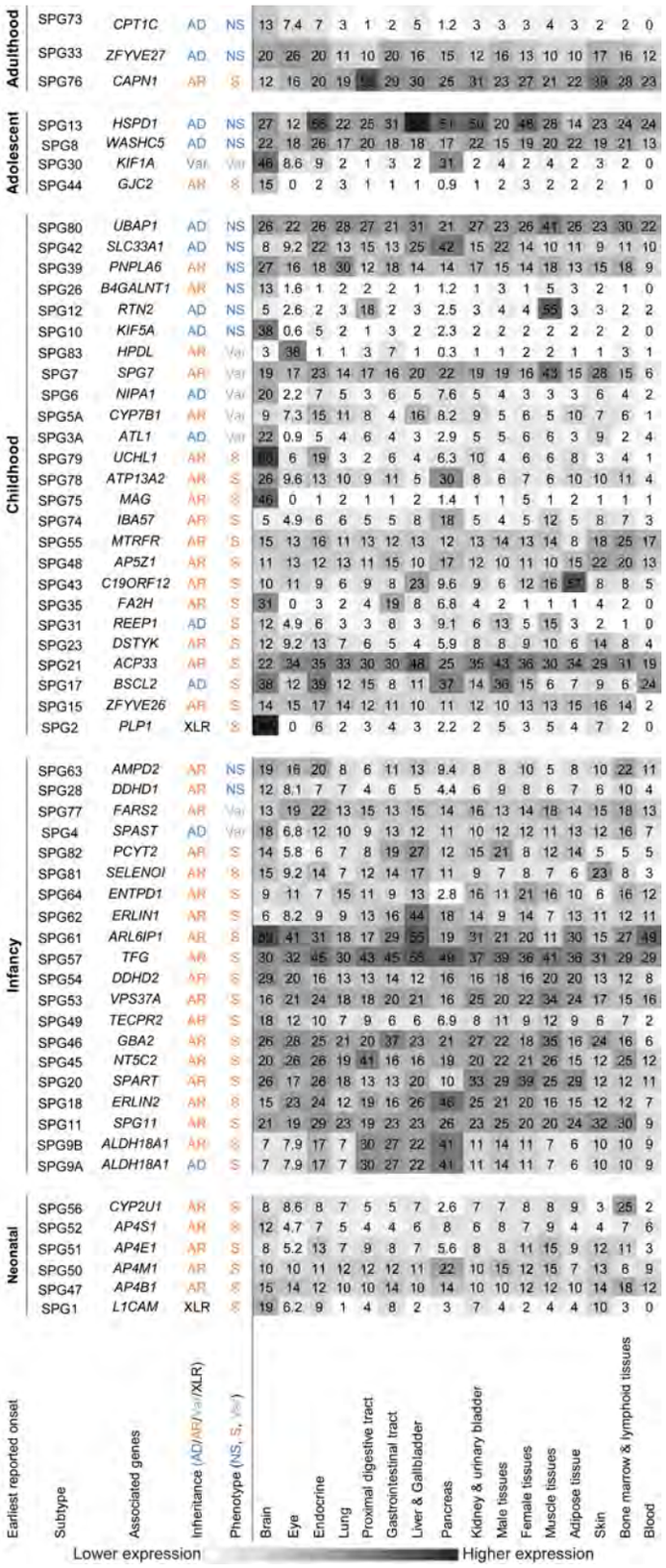

Figure 1 Heatmap showing average tissue-specific mRNA expression levels in transcripts per million (TPM) of HSP genes in normal human tissues (concise version of Supplementary Figure S5)

Each row specifies a generalized tissue type, and each column specifies the expression level in TPM of one HSP-associated gene. Columns are grouped with respect to earliest reported onset age of associated subtype. Metadata age of onset (neonatal, infancy, childhood, adolescent, adulthood), inheritance pattern (AD: Autosomal dominant; AR: Autosomal recessive; XLR: X-linked recessive; Var: Variable), and general phenotype (S: Syndromic; NS: Non-syndromic; Var: Variable) were based on documented records available in the literature. Tissue expression profile of each gene was retrieved from the Human Protein Atlas Database (v20) (Supplementary Figure S5) and averaged with respect to tissue type. Heatmap color intensity is positively correlated with average expression level.

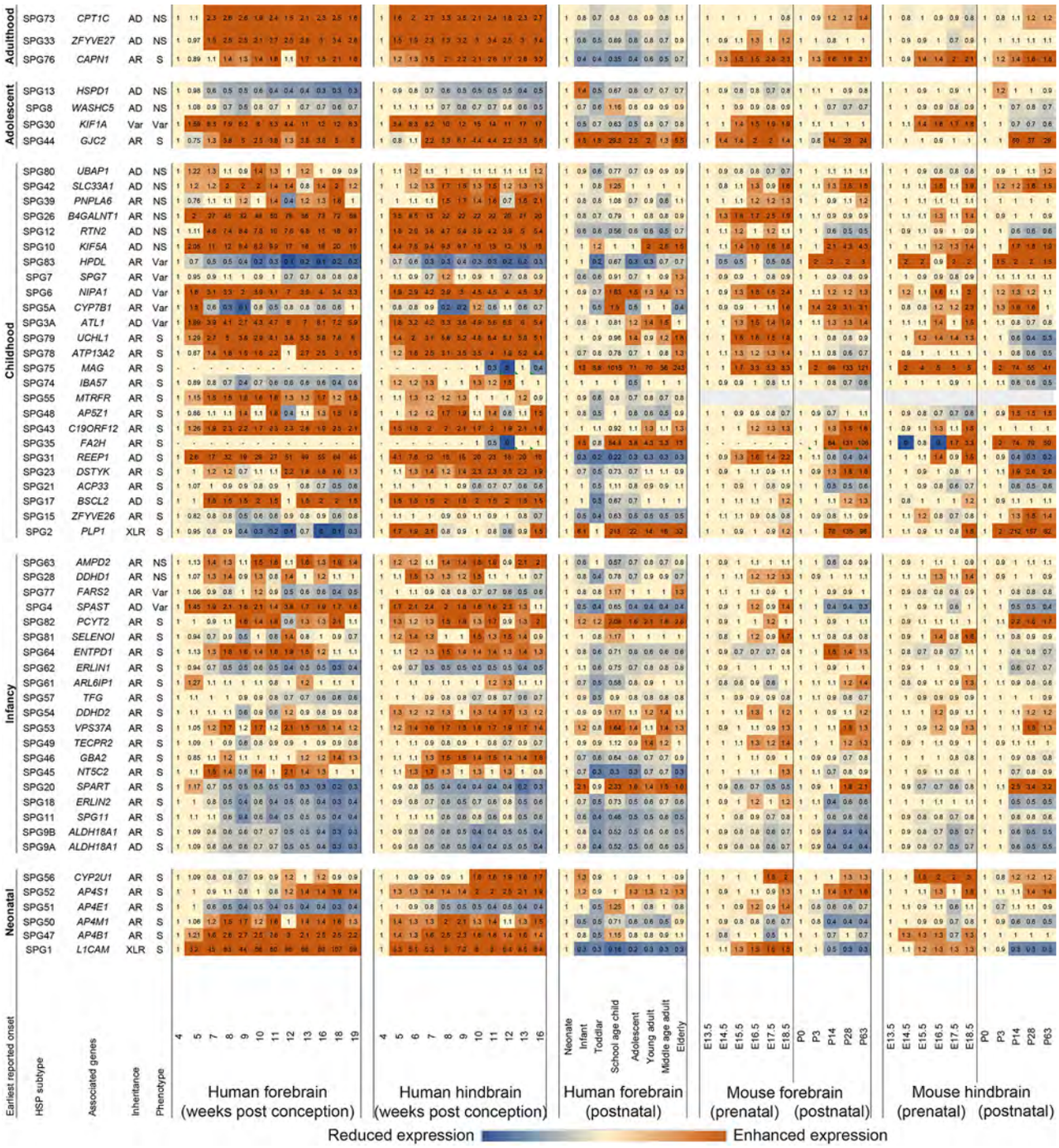

Figure 2 Heatmap showing relative mRNA expression profiles (TPM) of HSP genes in human and mouse forebrain and hindbrain

Each column specifies a timepoint and each row specifies the expression of an HSP-associated gene. Rows are grouped with respect to earliest reported onset. Reference timepoint of expression for each gene was defined as the first timepoint at which expression was detected at pre- and post-natal stages. Intensity of orange and blue indicates the extent to which expression increased or decreased, respectively.

forebrain and hindbrain; alternatively, the succeeding time point was referenced if expression was not detectable at this point. Similarly, neonatal expression, if detectable, was defined as the reference point for calculating relative fold-change in the postnatal human forebrain. The same process was applied for mouse expression data. To determine whether the profiles correlated with motor involvement in mouse models, the retrieved gene expression profiles were arranged based on whether equivalent HSP-gene mutations in mice led to phenotypic outcomes related to motor involvement as observed in humans (Figure 3) (Genc et al., 2019).

Single-cell transcriptome profiles of HSP genes

Cross-species motor cortex transcriptomic analysis was performed to identify specific cell types of interest (Bakken et al., 2021). Specifically, we extracted 10X scRNA-seq HSP-associated gene expression data in normal human M1 cortex (Allen Institute, 2021) (last accessed on 28 December 2021) (Supplementary Figure S2). The gene expression matrix data, processed into trimmed means, were subjected to dimensional analyses, including principal component analysis (PCA) and Uniform Manifold Approximation of Projection (UMAP) using the R packages “plotly” and “umap”, respectively (Figure 4;

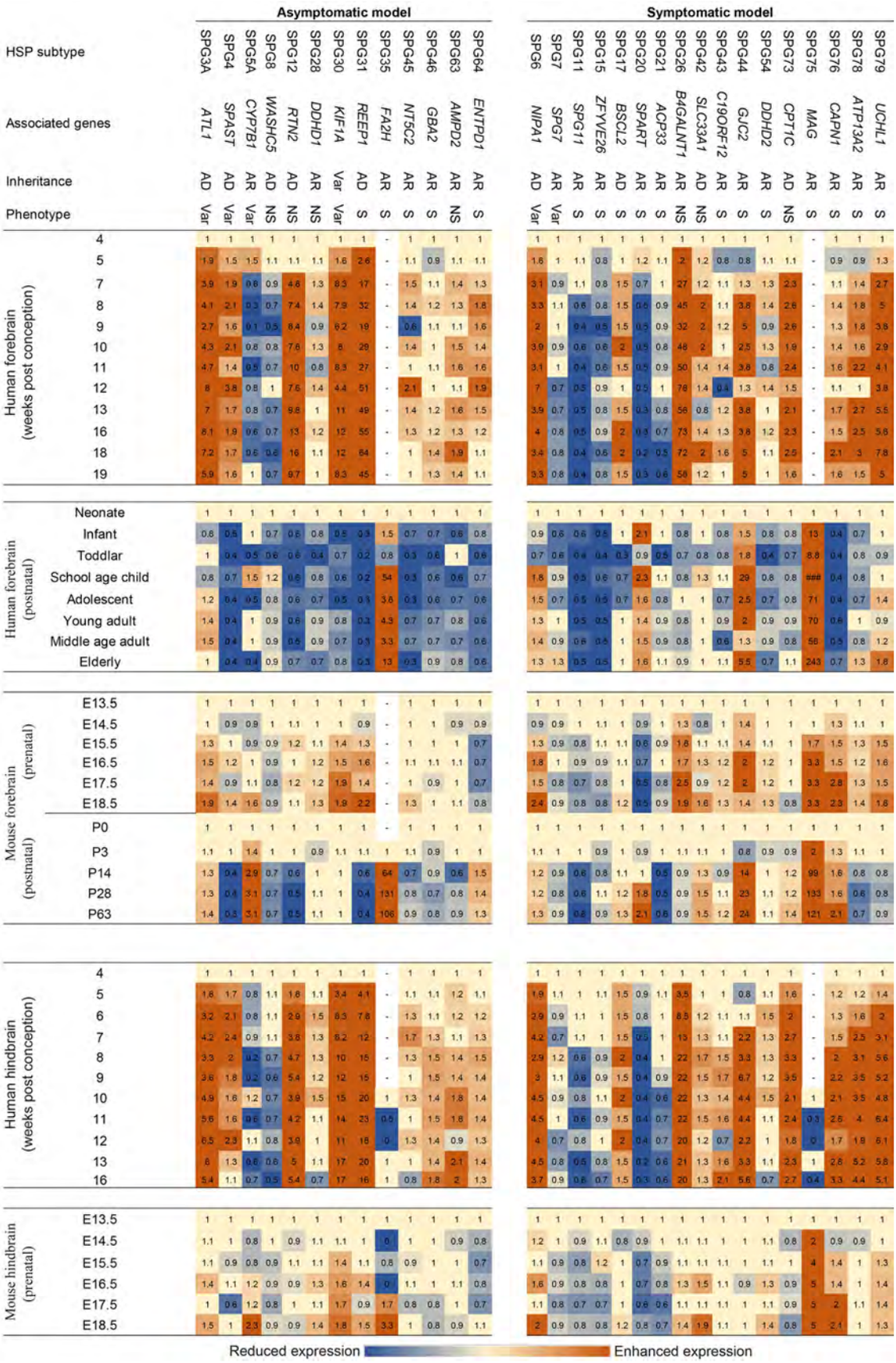

Figure 3 Heatmap comparing mRNA expression trends of HSP-associated genes in human and mouse forebrain/hindbrain across developmental stages

Each row specifies a timepoint and each column specifies log2 expression values relative to defined reference point (first detectable timepoint in Figure 2). Subtypes were grouped regarding whether mouse models showed phenotypes of cortical involvement. Blue indicates reduced expression and orange color indicates enhanced expression.

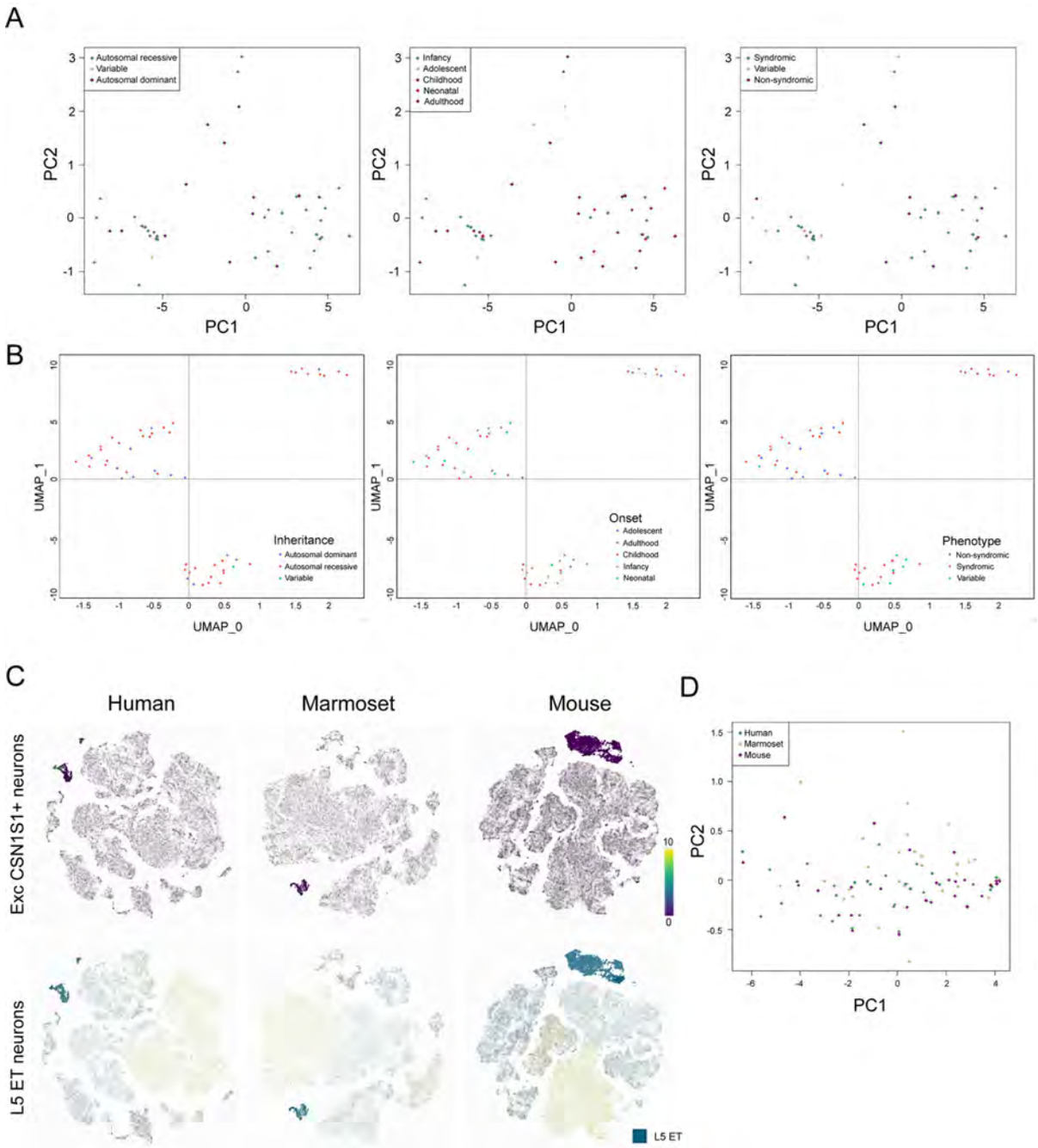

Figure 4 Dimensionality reduction analysis of transcriptomic cell-type-specific RNA-seq data

A: Dimensionality reduction by PCA and B: UMAP of scRNA-seq resulted HSP-gene expression profiles across selected pyramidal excitatory FEZF2+ neurons. C: Human CSN1S1+ neurons and equivalent populations in marmosets and mice are highlighted in purple, and layer 5 extratelencephalic (ET) populations in humans, marmosets, and mice are highlighted in blue. D: Dimensionality reduction by PCA of HSP-gene expression profiles in selected ET clusters across human, marmoset, and mouse snRNA-seq data.

Supplementary Figures S3, S4).

RESULTS AND DISCUSSION

Correlation between HSP gene expression and clinical presentation

Among the 71 reported subtypes (Supplementary Table S1), tissue-specific mRNA expression data were available in 58 HSP genes. We found that subtypes with the earliest reported age of onset during the neonatal period were all syndromic HSP (100%, 6/6). The syndromic:non-syndromic ratio of HSP subtypes decreased as the earliest reported onset age increased, i.e., a larger percentage of earlier onset HSP subtypes were syndromic. For instance, 80% of infancy (16/20), 56% of childhood (14/25), 25% of adolescent (1/4), and 33% of adulthood (1/3) onset HSP subtypes were syndromic (Figure 1). This may be because genes associated with neonatal onset HSP are more likely to play a pivotal role in growth and development than those associated with adulthood onset HSP, therefore affecting development and maturation of multiple associated regions in the brain, as shown in syndromic clinical presentation. For instance, Tüysüz et al. (2014) reported similar phenotypes for *AP4M1*-, *AP4E1*-, *AP4S1*-, and *AP4B1*-associated neonatal onset symptomatic

Table 1 Reported disease mechanisms and pLI scores of functionally characterized AD-HSP

HSP subtype			SPG3A	SPG4	SPG6	SPG10	SPG17	SPG30	SPG31	SPG42	SPG73
HGNC approved gene symbol			*ATL1*	*SPAST*	*NIPA1*	*KIF5A*	*BSCL2*	*KIF1A*	*REEP1*	*SLC33A1*	*CPT1C*
Inheritance pattern			AD	AD	AD	AD	AD	AD/AR	AD	AD	AD
Phenotype			Var	Var	Var	NS	S	Var	S	NS	NS
pLI score			0.981	0.999	0.006	1	0	1	0.986	0	0
Proposed mechanism	Dominant negative	*In vitro*	p.del436N[1]	p.K388R[2], p.L426V[2]	N/A	N/A	N/A	p.T258M[4]	N/A	p.S113R[1]	c.109C>T[2]
		In vivo	N/A	p.K467R[3]	N/A	p.N256S[3]	N/A	N/A	N/A	p.S113R[3]	c.109C>T[3]
	Loss-of-function (LoF)	*In vitro*	p.R217Q	p.Q193*[1], p.Q229*[1], c.1634del22[1], p.C448Y[1]	p.T39R[4], p.G100R[4]	N/A	N/A	N/A	N/A	N/A	N/A
		In vivo	N/A	N/A	N/A	N/A	N/A	N/A	p.I57S[3], p.F58S[3], p.F62S[3], p.F64S[3]	N/A	N/A
	Gain-of-toxic-function (GoF)	*In vitro*	N/A	N/A	N/A	N/A	p.N88S[2], p.S90L[2]	N/A	N/A	N/A	N/A

Disease-causing variants of AD-HSP subtypes were retrieved from previous literature and tabulated with reference to disease mechanisms. N/A: Not available. 1: Cells from patients, 2: Multiple cell lines not from patients, 3: Species-specific expression (e.g.: *Drosophila Spast* and *Kif5a* in *Drosophila* model for SPG4 and SPG10 characterization, mice *Reep1* in mouse model for SPG31 characterization), 4: Non-species-specific expression: (e.g.: mouse *Nipa1* in *Xenopus* oocytes for SPG6 characterization, mouse *Kif1a* in rat hippocampal neurons for SPG30 characterization).

HSP subtypes, with brain imaging of three families affected by these subtypes revealing shared abnormalities, including asymmetrical ventriculomegaly, reduction in white matter volume, and thinning of corpus callosum splenium; however, these structural abnormalities are not observed in later onset non-symptomatic HSP subtypes, such as the *UBAP1*-associated SPG80 (Fard et al., 2019).

It is difficult to quantify reported phenotypes of each HSP subtype due to varying assessment methodologies and documentation. Nevertheless, phenotypic outcomes of HSP appear to be associated with age. Based on the literature, 100% of neonatal onset HSP subtypes are associated with intellectual disability (ID) (Gareis et al., 1984; Kaepernick et al., 1994; Winter et al., 1989). While XLR-SPG1 patients usually present with mild ID, patients of the other 80% (4/5) neonatal onset AR-HSP subtypes are associated with severe ID. The degree of severity for the remaining SPG56 subtype varies. Unlike other forms of neonatal onset HSP (earliest reported), in which disease phenotypes usually present at birth (Abdollahpour et al., 2015; Jamra et al., 2011; Tüysüz et al., 2014), the age of onset of SPG56 ranges from birth to 8 years (Pujol et al., 2021; Tesson et al., 2012). In total, 69% (11/16) of infancy-onset syndromic HSP subtypes are associated with ID to varying degrees, ranging from mild to moderate. Only SPG9B (Coutelier et al., 2015), SPG18 (Al-Saif et al., 2012; Yıldırım et al., 2011), SPG49 (Heimer et al., 2016; Neuser et al., 2021), and SPG82 (Vaz et al., 2019) cause varying levels of severely impaired intellectual development. Among the childhood-onset HSP subtypes, 54% (7/13) present with intellectual decline or ID, mostly mild, with only SPG75 involving mild to moderate ID (Lossos et al., 2015). Only one adolescent-onset HSP subtype and one adulthood-onset HSP subtype are syndromic. Notably, adolescent-onset SPG44 exhibits mild intellectual involvement, which is described as mild learning disability (Orthmann-Murphy et al., 2009), whereas intellectual involvement in adulthood-onset syndromic SPG76 is not reported (Gan-Or et al., 2016). While the extent of intellectual involvement in syndromic HSP appeared to decline with increasing age of onset, the spectrum of other reported clinical features varied the most for infancy- and childhood-onset HSP, ranging from visual and hearing involvement, loss of teeth, autonomic dysfunction, testicular hypotrophy to canities.

A much larger percentage of AR-HSP subtypes (~80%, 33/41) are syndromic, in contrast to AD-HSP subtypes (~21%, 3/14). This may be because nearly all AR disorders result from loss-of-function (LoF) of the disease gene, which renders both copies of the gene non-functional or reduces/eliminates gene expression (Veitia et al., 2018). Thus, functional defects in AR diseases are likely to be more universal compared to AD disorders, in which only one copy of the gene carries the deleterious change. As a result, it is feasible that AD-HSP genes may still function at a lower but adequate level in some tissues and organs.

Based on literature, eight out of 14 AD-HSP subtypes and AD/AR-HSP SPG30 have been functionally characterized *in vitro* and/or *in vivo* (Table 1). In general, pathogenicity of the AD-HSP subtypes result from dominant-negative LoF or gain-of-function (GoF) disease mechanisms. Disease mechanisms of certain variants causing SPG10 (Füger et al., 2012), SPG30 (Cheon et al., 2017), SPG42 (Mao et al., 2015), and SPG73 are identified as dominant-negative, while that of SPG17 is identified as GoF (Ito & Suzuki, 2007). The pathological mechanisms of SPG6 (Goytain et al., 2007) and SPG31 (Beetz et al., 2013) attributes to LoF, while both LoF and dominant-negative variants are reported for SPG3A (Meijer et al., 2007; Muglia et al., 2002) and SPG4 (Charvin et al., 2003; Errico et al., 2002; Orso et al., 2005). Although the functional characterization of disease-causing variants associated with SPG8 has been explored (Clemen et al., 2022; Song et al., 2018), no clear conclusion have been drawn. Furthermore, despite exclusion of the GoF mechanism, no conclusion have been drawn regarding the pathogenicity of SPG12 (Montenegro et al., 2012). Similarly, no disease mechanism has been defined for SPG9 (Panza et al., 2016), SPG13 (Bross & Fernandez-Guerra, 2016), SPG33 (Mannan et al., 2006), or SPG80 (Fard et al., 2019; Gu et al., 2020). The pLI scores for each of the characterized AD-SPG genes are indicated in Table 1. The pLI score reflects the tolerance of a given gene to LoF changes by comparing expected

versus observed LoF variants (Karczewski et al., 2020), with a higher pLI implying that the gene is less tolerant to LoF variants, and vice versa. We observed that genes associated with LoF-induced AD-HSP, i.e., *ATL1* (SPG3A), *SPAST* (SPG4), and *REEP1* (SPG31), showed high pLI scores (Table 1), while that of *NIPA1* (SPG6) was very low (pLI=0.006). The proposed LoF *Nipa1* variants have been evaluated by expressing mouse *Nipa1* in *Xenopus* oocytes and endogenous expression of the Nipa1 protein in the mouse MDCT cell line (Goytain et al., 2007). The low pLI score of *NIPA1* suggests additional analysis is warranted to define the LoF mechanism.

Once disease mechanisms are identified through functional characterization experiments, the primary targets for pharmaceutical development can be determined. For GoF diseases, which exhibit novel functions not present in healthy cells, a target-based drug design model is effective for developing management or curative measures (Ségalat, 2007). This approach can also be applied to LoF diseases when the targets have well-understood physiopathology or are involved in metabolic diseases (Ségalat, 2007). However, for dominant-negative diseases, target-based drug development may be difficult, even after thorough functional characterization. As illustrated in Table 1, the dominant-negative disease mechanism is frequently associated with AD-HSP. Therefore, novel approaches are needed for functional characterization of gene variants associated with dominant-negative AD-HSP to facilitate the development of effective management and treatment strategies.

Inter-species relevance of HSP gene expression profile

Gene expression patterns along developmental stages varied considerably by gene and species (Figure 2; Supplementary Figure S1). Examples of HSP genes showing distinct expression patterns across species included *REEP1*, *SPAST*, *HPDL*, *FA2H*, and *MAG*. In human forebrain tissues, *REEP1* and *SPAST* expression levels enhance prenatally and decrease postnatally. *HPDL* expression decreases from 20 TPM to 3 TPM prenatally (4–19 wpc) and from 3 TPM to 0.8–2 TPM postnatally. In contrast, *GJC2* expression increases from 0.8 TPM to 19 TPM prenatally (4–19 wpc) and from 4 TPM to 22 TPM postnatally. Some genes, such as *FA2H* and *MAG*, do not express in the forebrain, but are merely detectable after 10 wpc in the hindbrain during prenatal periods. Their expression in the forebrain and hindbrain, however, is significantly higher during postnatal periods.

Both the expression trend during development and differential expression levels between tissue/cell types contributed to data heterogeneity. *In vivo* experiments are often used to aid investigations, with mice being the most commonly used organism in preclinical studies, including research on human neurodegenerative diseases (Vandamme, 2014). Focusing on interspecies differences based on genetic background, Genc et al. (2019) investigated mouse models that mimic genetic changes in human HSP genes to determine whether they exhibit similar phenotypes of upper motor neuron involvement, as observed in human patients. Notably, however, not all mouse models showed motor involvement. To investigate whether differential cross-species HSP gene expression profiles are associated with motor-involvement phenotypes in mice, the retrieved expression profiles in this study were arranged according to whether equivalent HSP gene mutations in mice led to phenotypic outcomes related to motor involvement, as in human patients (Figure 3). The presentation of cortical involvement phenotypes was not correlated with the similarity of expression differences between humans and mice, both prenatally and postnatally. For example, *ENTPD1*-associated SPG64 displays an AR inheritance, indicating the disease is likely due to *ENTPD1* LoF changes, while disruption of *ENTPD1* in mice fails to develop HSP-related phenotypes (Genc et al., 2019). Although *ENTPD1*-disrupted models are not initially developed to model HSP (Enjyoji et al., 1999; Friedman et al., 2007), it should be noted that *ENTPD1* expression between humans and mice showed the opposite trend. The expression trends of *CYP7B1*-associated childhood-onset AR-SPG5A also showed differences. The postnatal expression of *CYP7B1* is generally suppressed in humans but enhanced in mice (Figure 3). While the AR pattern of inheritance indicates that LoF would likely be the disease mechanism, no HSP-related symptoms have been reported in *CYP7B1*-disrupted mouse models (Genc et al., 2019). Additionally, although the expression trend of *WASHC5* was very similar between humans and mice, according to the literature, the *WASHC5*-associated SPG8 mouse model still fails to display HSP-related phenotypes (Jahic et al., 2015). The limitations of mouse models in degenerative motor neuron disease (MND) research are potentially attributed to differences in the complexity of motor neuron circuitry between humans and mice (Genc et al., 2019). CSMNs receive multiple cortical inputs from layer 5 and more superficial layers along their long apical dendrites via dendritic spines (Genc et al., 2019). Although the synaptic densities targeting the dendritic shaft of pyramidal cells are relatively constant across species in layer 2/3, the density of synapses targeting the dendritic spines of pyramidal cells is significantly lower in humans than in mice (Loomba et al., 2022). Furthermore, differential inhibitory/excitatory balance along the dendritic shafts of pyramidal cells between humans and mice is reported (Loomba et al., 2022). These differential connectomic circuitries in the central nervous system (CNS) between humans and mice may explain the differential phenotypic outcomes in some documented mouse models (Genc et al., 2019). In addition, a much higher level of similarities in terms of cortical circuitry between human and macaques than with mice has been revealed from comparative connectomic analyses between macaques, humans, and mice (Loomba et al., 2022). As a result, we further investigated the expression patterns of HSP genes in non-human primates based on a study of 547 transcriptomes from 44 anatomical brain areas of rhesus macaques (Li et al., 2019). Average expression of HSP genes in the cortical areas of rhesus macaques were tabulated by age; however, no significant differences or trends were observed across young or older subjects (Supplementary Table S2). Additional time points may be required for more thorough comparison. Therefore, cross-species similarity in terms of gene expression during development may not be valuable for predicting cross-species phenotypic outcomes in HSP.

Potential implications of HSP genes in association with other neurodegenerative diseases

HSP associated variants in *PLP1*, *HSPD1*, and *GJC2* cause different types of hypomyelinating leukodystrophies (Matsumoto et al., 2019) (Supplementary Table S1), alongside childhood-onset syndromic SPG2, adolescent-onset non-syndromic SPG13, and syndromic SPG44, respectively.

Specifically, *PLP1* is associated with X-linked prototypic hypomyelinating leukodystrophy 1 (HLD1) (Matsumoto et al., 2019), *GJC2* with hypomyelinating leukodystrophy 2 (HLD2) (Komachali et al., 2022), and HSPD1 with hypomyelinating leukodystrophy 4 (HLD4) (Cömert et al., 2020). Regarding their expression patterns (Figure 2), prenatal expression of *PLP1* shows a generally decreasing trend in the forebrain and alternating trends in the hindbrain; postnatal expression of *PLP1* demonstrates an increasing trend in the forebrain, which peaks between toddler age and adolescence. Prenatal expression of *HSPD1* in both the forebrain and hindbrain generally decrease with time, while postnatal expression of *HSPD1* in the forebrain also decreases after a peak during infancy. Prenatal and postnatal expression of *GJC2* in both the forebrain and hindbrain generally follows an increasing trend. Thus, the expression profiles of these genes were quite distinct, even though they all lead to HLD. The *TFG* (Tsai et al., 2014) and *SPG11* genes (Montecchiani et al., 2016) are associated with Charcot-Marie-Tooth (CMT) disease type 2 (Supplementary Table S1), alongside infancy-onset syndromic SPG57 and SPG11, respectively. The expression profiles of *TFG* and *SPG11* demonstrated similar trends, variously decreasing with time during both the pre- and postnatal periods. The *C19ORF12* (Deschauer et al., 2012) and *ATP13A2* genes (Kruer et al., 2012), which cause childhood-onset syndromic SPG43 and SPG78, respectively, are also causing brain iron accumulation-associated neurodegeneration (Supplementary Table S1). The expression profiles of *C19ORF12* and *ATP13A2* exhibited similar trends, increasing prenatally and remaining rather stable postnatally.

CYP7B1, *KIF5A*, *RTN2*, and *REEP1* are differentially expressed in the pathological models of Alzheimer's diseases (Supplementary Table S3). They are associated with childhood-onset SPG5A with variable phenotype, non-syndromic SPG10 and SPG12, and syndromic SPG31, respectively. Regarding their expression patterns (Figure 2), all showed a similar increasing trend during prenatal periods, except for *CYP7B1*, which showed a generally decreasing trend. The postnatal expression levels of *CYP7B1* between humans and mice were markedly different from each other. Thus, no consistent expression trend could be identified for genes implicated in Alzheimer's disease.

Single-cell transcriptome profiles of HSP genes

According to the brain tissue mRNA expression data presented in Supplementary Figure S5, most HSP genes exhibited low brain specificity in expression profiles, suggesting that many HSP genes are ubiquitously expressed in the brain. However, based on clinical presentation in non-syndromic HSP subtypes, only CSMNs appear to be affected. Therefore, using bulk mRNA expression measured across each tissue type may not be sufficient to accurately depict molecular pathogenicity restricted to a very specific cellular population. For example, projection neurons alone contain hundreds of transcriptomically differentiable cellular subtypes, each with a distinct gene expression profile (Yao et al., 2021). Although bulk RNA-seq permits general transcriptomic analysis, it only produces average expression data, which may obscure the expression profiles of specific cell populations of interest (Hwang et al., 2018). HSP involves upper motor neurons in the pyramidal tract, primarily FEZF2+ layer 5 glutamatergic motor neurons (Deng et al., 2021). Analysis of single-nucleus RNA-seq (snRNA-seq)/scRNA-seq data from postmortem human primary motor cortex and mouse isocortex and hippocampal specimens (Allen Institute, 2021), as well as Patch-seq data, i.e., patch-clamp and scRNA sequencing to obtain electrophysiological and transcriptomic information from the same individual neuron, from mouse motor cortex samples (Scala et al., 2021), revealed the presence of a wide range of transcriptomic cell types, even within the FEZF2+ glutamatergic population. Thus, the emergence of scRNA-seq technology allows researchers to refine the resolution of gene expression data from the tissue to cellular level via single-cell transcriptomic profiles.

We extracted 10X scRNA-seq HSP-associated gene expression data from all characterized cell types in normal human M1 cortex (Allen Institute, 2021) (last accessed on 28 December 2021) (Supplementary Figure S2). To refine the populations for further analysis, PCA was performed on HSP gene expression levels in all human pyramidal tract (PT) excitatory neurons, followed by clustering based on disease-related characteristics (Supplementary Figure S3A). The weightings of each transcriptomic cell type contributing to variance across the two PCA dimensions were then subjected to cos2 analysis (Supplementary Figure S3B). Results showed that FEZF2+ excitatory neurons that were also PROKR2+, OR1L8+, LPO+, ASGR2+, or CSN1S1+ were the top five contributing neuronal cell types. Interestingly, previous research has shown that the FEZF2+ ASGR2+ and FEZF2+ CSN1S1+ excitatory neurons exhibit CSMN signatures (Bakken et al., 2021). The HSP-gene transcriptomic profiles in the five selected FEZF2+ excitatory neurons were subjected to dimensionality reduction analysis by PCA and UMAP. After PCA (Figure 4A), no clustering based on general phenotype, inheritance pattern, or earliest reported age of onset was identified. Similarly, no clustering was observed among expression profiles of HSP genes in selected mouse isocortical pyramidal tract (PT.CTX) neurons (Supplementary Figure S4A). However, UMAP analysis revealed that while gene expression profiles did not cluster by HSP phenotypic characteristics, they formed into three distinct clusters in human postmortem motor cortex specimens (Figure 4B) and mouse isocortex and hippocampal specimens (Supplementary Figure S4B). This may be due to the non-linear nature of UMAP, which can reveal the structure beyond the linear relationship considered by PCA. However, the non-linear nature of UMAP disconnects the data point from linear algebra, and the weighting of components in each axis cannot be computed. The clustering observed in our study may be due to similarity in expression patterns across selected transcriptomic cell types. Similar dimensionality reduction analysis was conducted for various neuronal populations, however no significant results were identified (data not shown). We speculate that currently available scRNA-seq/snRNA-seq data from healthy subjects do not meet the requirements for the delineation of molecular pathology in diseases involving very specific cell type(s), such as degeneration of CSMN in HSP. Thus, scRNA-seq and snRNA-seq analyses of more restricted brain regions from diseased subjects are integral for future HSP mechanistic studies.

To further investigate the reason why motor defects as in HSP patients may not present in a certain mouse models (Genc et al., 2019), the expression profiles of HSP genes in a subset of transcriptomic neuronal populations from humans and mice were subjected to PCA. Normalized cross-species

single-cell expression levels in human, mouse, and marmoset brains were generated from online repositories, including the Allen Brain Institute cell type database (Allen Institute, 2021), Neuroscience Multi-Omic Analytics browser (Orvis et al., 2021), and other sources indicated below (Bakken et al., 2021; Scala et al., 2021). HSP gene expression profiles in human L5 excitatory ET populations, which encompass FEZF2+ CSN1S1+ and FEZF2+ ASGR2+ neurons, together with their equivalent populations in mice and marmosets (Bakken et al., 2021) (Figure 4C) were obtained via Cytosplore (Supplementary Table S4) for PCA (Figure 4D). No distinct species-specific clustering of HSP gene expression profiles was identified. The expression of HSP genes during development, as well as their transcriptomic-specific expression across species, did not distinguish the HSP mouse models in terms of whether or not they exhibited motor defects. This may be due to divergent neuronal networking between humans and mice. While some upper motor neurons in humans allow signal propagation directly onto spinal motor neurons, these signals in rodents propagate indirectly via spinal interneurons (Lemon, 2008). Therefore, rodents may not be suitable species for constructing preclinical models for some HSP genes.

To date, the molecular complexity of HSP remains poorly understood and no research on this inheritable MND has yet been conducted using single-cell transcriptomic analysis. Furthermore, the neuropathic mechanism of CSMN in HSP remains largely unknown. However, several transcriptomic studies using scRNA-seq have been conducted to delineate the molecular mechanisms underlying amyotrophic lateral sclerosis (ALS), which involves degeneration of both the upper and lower motor neurons (Ho et al., 2021; Liu et al., 2020; Namboori et al., 2021; Saez-Atienzar et al., 2021). Based on a PubMed literature search, no other MND appears to have been investigated using single-cell techniques.

Studies on ALS have conducted scRNA-seq and snRNA-seq based on a widely used ALS-*SOD1* transgenic mouse model (Cohen et al., 2021; Liu et al., 2020; MacLean et al., 2022; Mifflin et al., 2021; Yim et al., 2022). Other studies have performed scRNA-seq on patient-derived organoids (Ho et al., 2021; Namboori et al., 2021; Szebényi et al., 2021) and spatial transcriptomic analysis of patient-derived postmortem cortical tissues (Gregory et al., 2020). ScRNA-seq/snRNA-seq analysis of specimens from various CNS regions in *SOD1*-ALS mice reveals transcriptomic alterations in most cell types in the brainstem (Liu et al., 2020) and involvement of distinct inflammatory responses in the spinal cord (Cohen et al., 2021; Mifflin et al., 2021), which may associate with disturbed neuronal-glial communication (MacLean et al., 2022). In addition, the identification of the inflammatory microglial subclass associated with ALS motor neuron degeneration has led to the discovery that its suppression can provide therapeutic benefit in *SOD1*-ALS-diseased mice (Mifflin et al., 2021). As investigations into MND pathology in humans are limited by the availability of patient specimens, scRNA-seq of human patient cell-derived motor nerve organoids has revealed unified and reproducible early motor neuron-resolved ALS signatures (Ho et al., 2021; Namboori et al., 2021), as well as rescuable involvement of astroglia-mediated disease pathways (Szebényi et al., 2021). These transcriptomic studies have laid the foundation for understanding the pathogenesis of ALS in terms of spatial and molecular specificity, enabling further improvement in ALS management. Similar strategies may benefit HSP research and treatment in the future, more specifically, in cases where rodent models may not be able to recapitulate human HSP phenotypic outcomes.

Limitations

As the expression profiles of HSP genes were obtained from heterogeneous sources, this study has several limitations. For instance, although normalized bulk RNA-seq data from the Human Protein Atlas v20 were analyzed, they were acquired from different cohorts with unknown genetic background. Furthermore, while this review article interpreted and summarized the clinical and molecular features of HSP in terms of mode of inheritance, HSP gene expression, potential mechanisms, and reported onset ages of various HSP subtypes, additional extrinsic and intrinsic factors related to patient lives may contribute to disease onset, progression, and severity, which are beyond the scope of our analysis.

CONCLUSIONS

Based on our HSP gene expression profile analysis, HSP subtypes with earlier onset age were more likely to result in clinical presentation of syndromic HSP. In addition, HSP-associated genes inherited in an AR manner were more likely to cause syndromic HSP than AD subtypes. Differential gene expression patterns of HSP genes in the normal primary motor cortex of the human brain were not correlated with general phenotype, inheritance pattern, or age of onset of HSP subtype. Differential transcriptomic subtype-specific expression and expression trends with development did not serve as indicators of cross-species HSP phenotypic outcome. Therefore, although numerous HSP genes have been identified, our understanding of the molecular mechanisms underlying disease presentation and progression is still extremely limited. Current research obstacles include the lack of patient transcriptomic data and molecular complexity/transcriptomic diversity of cell types in the brain. As demonstrated by recent advancements in ALS characterization, coupling patient cell-derived organoid cultures or diseased mouse models with scRNA-seq technologies may be the key to decoding HSP pathogenicity at cellular resolution.

DATA AVAILABILITY

The HSP genes used in this study are available via the OMIM PS303350 phenotypic series (https://omim.org/phenotypicSeries/PS303350) (last accessed on 14 September 2021). The tissue-specific transcriptomic datasets analyzed in this study are available via the v20 Human Protein Atlas portal (https://v20.proteinatlas.org/) (last accessed on 14 November 2021). The expression data with developmental time are accessible via the EMBL-EBI Expression Atlas portal (https://www.ebi.ac.uk/gxa/home) (last accessed on 11 December 2021). The scRNA-seq datasets are available from the Allen Institute cell-type database (RNA-Seq Data) (https://portal.brain-map.org/atlases-and-data/rnaseq) (last accessed on 28 December 2021). The mouse motor cortical Patch-seq dataset is available at GitHub (https://github.com/berenslab/mini-atlas) (last accessed on 9 June 2022). The cross-species snRNA-seq dataset is available via Cytosplore Viewer (https://viewer.cytosplore.org/) (last accessed on 10 June 2022). The pLI scores are available from the gnomAD browser (https://gnomad.broadinstitute.org/) (last accessed on 20 May 2022). The CFG scores of HSP genes are available from the AlzData database (http://alzdata.org/) (last accessed on 24 November 2022).

SUPPLEMENTARY DATA

Supplementary data to this article can be found online.

COMPETING INTERESTS

The authors declare that they have no competing interests.

AUTHORS' CONTRIBUTIONS

N.J.H. acquired, analyzed, and interpreted the data. N.J.H. and S.G. designed the study and wrote the manuscript. X.C. and Y.L. conceived, critically revised, and supervised the work. All authors read and approved the final version of the manuscript.

REFERENCES

Abdollahpour H, Alawi M, Kortum F, et al. 2015. An AP4B1 frameshift mutation in siblings with intellectual disability and spastic tetraplegia further delineates the AP-4 deficiency syndrome. *European Journal of Human Genetics*, **23**(2): 256−259.

Al-Saif A, Bohlega S, Al-Mohanna F. 2012. Loss of *ERLIN2* function leads to juvenile primary lateral sclerosis. *Annals of Neurology*, **72**(4): 510−516.

Allen Institute. 2021. Cell types database: RNA-Seq data.https://portal.brain-map.org/atlases-and-data/rnaseq.

Bakken TE, Jorstad NL, Hu QW, et al. 2021. Comparative cellular analysis of motor cortex in human, marmoset and mouse. *Nature*, **598**(7879): 111−119.

Beetz C, Koch N, Khundadze M, et al. 2013. A spastic paraplegia mouse model reveals REEP1-dependent ER shaping. *The Journal of Clinical Investigation*, **123**(10): 4273−4282.

Bellofatto M, De Michele G, Iovino A, et al. 2019. Management of hereditary spastic paraplegia: a systematic review of the literature. *Frontiers in Neurology*, **10**: 3.

Bross P, Fernandez-Guerra P. 2016. Disease-associated mutations in the *HSPD1* gene encoding the large subunit of the mitochondrial HSP60/HSP10 chaperonin complex. *Frontiers in Molecular Biosciences*, **3**: 49.

Cardoso-Moreira M, Halbert J, Valloton D, et al. 2019. Gene expression across mammalian organ development. *Nature*, **571**(7766): 505−509.

Charvin D, Cifuentes-Diaz C, Fonknechten N, et al. 2003. Mutations of SPG4 are responsible for a loss of function of spastin, an abundant neuronal protein localized in the nucleus. *Human Molecular Genetics*, **12**(1): 71−78.

Cheon CK, Lim SH, Kim YM, et al. 2017. Autosomal dominant transmission of complicated hereditary spastic paraplegia due to a dominant negative mutation of *KIF1A*, SPG30 gene. *Scientific Reports*, **7**(1): 12527.

Clemen CS, Schmidt A, Winter L, et al. 2022. N471D WASH complex subunit strumpellin knock-in mice display mild motor and cardiac abnormalities and BPTF and KLHL11 dysregulation in brain tissue. *Neuropathology and Applied Neurobiology*, **48**(1): e12750.

Cohen M, Giladi A, Raposo C, et al. 2021. Meningeal lymphoid structures are activated under acute and chronic spinal cord pathologies. *Life Science Alliance*, **4**(1): e202000907.

Cömert C, Brick L, Ang D, et al. 2020. A recurrent de novo *HSPD1* variant is associated with hypomyelinating leukodystrophy. *Cold Spring Harbor Molecular Case Studies*, **6**(3): a004879.

Coutelier M, Goizet C, Durr A, et al. 2015. Alteration of ornithine metabolism leads to dominant and recessive hereditary spastic paraplegia. *Brain*, **138**(Pt 8): 2191–2205.

De Souza PVS, De Rezende Pinto WBV, De Rezende Batistella GN, et al. 2017. Hereditary spastic paraplegia: clinical and genetic hallmarks. *The Cerebellum*, **16**(2): 525−551.

DeLuca GC, Ebers GC, Esiri MM. 2004. The extent of axonal loss in the long tracts in hereditary spastic paraplegia. *Neuropathology and Applied Neurobiology*, **30**(6): 576−584.

Deng HF, Xiao X, Yang T, et al. 2021. A genetically defined insula-brainstem circuit selectively controls motivational vigor. *Cell*, **184**(26): 6344−6360.e18.

Deschauer M, Gaul C, Behrmann C, et al. 2012. *C19orf12* mutations in neurodegeneration with brain iron accumulation mimicking juvenile amyotrophic lateral sclerosis. *Journal of Neurology*, **259**(11): 2434−2439.

Enjyoji K, Sévigny J, Lin Y, et al. 1999. Targeted disruption of *cd39*/ATP diphosphohydrolase results in disordered hemostasis and thromboregulation. *Nature Medicine*, **5**(9): 1010−1017.

Errico A, Ballabio A, Rugarli EI. 2002. Spastin, the protein mutated in autosomal dominant hereditary spastic paraplegia, is involved in microtubule dynamics. *Human Molecular Genetics*, **11**(2): 153−163.

Fard MAF, Rebelo AP, Buglo E, et al. 2019. Truncating mutations in *UBAP1* cause hereditary spastic paraplegia. *The American Journal of Human Genetics*, **104**(6): 1251.

Friedman DJ, Rennke HG, Csizmadia E, et al. 2007. The vascular ectonucleotidase ENTPD1 is a novel renoprotective factor in diabetic nephropathy. *Diabetes*, **56**(9): 2371−2379.

Füger P, Sreekumar V, Schule R, et al. 2012. Spastic paraplegia mutation N256S in the neuronal microtubule motor KIF5A disrupts axonal transport in a *Drosophila* HSP model. *PLoS Genetics*, **8**(11): e1003066.

Gan-Or Z, Bouslam N, Birouk N, et al. 2016. Mutations in *CAPN1* cause autosomal-recessive hereditary spastic paraplegia. *The American Journal of Human Genetics*, **98**(5): 1038−1046.

Gareis FJ, Mason JD, Opitz JM. 1984. X-linked mental retardation associated with bilateral clasp thumb anomaly. *American Journal of Medical Genetics*, **17**(1): 333−338.

Genc B, Gozutok O, Ozdinler PH. 2019. Complexity of generating mouse models to study the upper motor neurons: let us shift focus from mice to neurons. *International Journal of Molecular Sciences*, **20**(16): 3848.

Goytain A, Hines RM, El-Husseini A, et al. 2007. *NIPA1(SPG6)*, the basis for autosomal dominant form of hereditary spastic paraplegia, encodes a functional Mg^{2+} transporter. *The Journal of Biological Chemistry*, **282**(11): 8060−8068.

Gregory JM, McDade K, Livesey MR, et al. 2020. Spatial transcriptomics identifies spatially dysregulated expression of *GRM3* and *USP47* in amyotrophic lateral sclerosis. *Neuropathology and Applied Neurobiology*, **46**(5): 441−457.

Gu S, Chen CA, Rosenfeld JA, et al. 2020. Truncating variants in *UBAP1* associated with childhood-onset nonsyndromic hereditary spastic paraplegia. *Human Mutation*, **41**(3): 632−640.

Gumeni S, Vantaggiato C, Montopoli M, et al. 2021. Hereditary spastic paraplegia and future therapeutic directions: beneficial effects of small compounds acting on cellular stress. *Frontiers in Neuroscience*, **15**: 660714.

Hedera P. 1993. Hereditary spastic paraplegia overview. *In*: Adam MP, Everman DB, Mirzaa GM, Pagon RA, Wallace SE, Bean LJH, et al. GeneReviews®. Seattle: University of Washington.

Heimer G, Oz-Levi D, Eyal E, et al. 2016. *TECPR2* mutations cause a new subtype of familial dysautonomia like hereditary sensory autonomic neuropathy with intellectual disability. *European Journal of Paediatric Neurology*, **20**(1): 69−79.

Ho R, Workman MJ, Mathkar P, et al. 2021. Cross-comparison of human iPSC motor neuron models of familial and sporadic ALS reveals early and convergent transcriptomic disease signatures. *Cell Systems*, **12**(2): 159−175.e9.

Hwang B, Lee JH, Bang D. 2018. Single-cell RNA sequencing technologies and bioinformatics pipelines. *Experimental & Molecular Medicine*, **50**(8): 1−14.

Ito D, Suzuki N. 2007. Molecular pathogenesis of seipin/BSCL2-related motor neuron diseases. *Annals of Neurology*, **61**(3): 237−250.

Jahic A, Khundadze M, Jaenisch N, et al. 2015. The spectrum of *KIAA0196* variants, and characterization of a murine knockout: implications for the mutational mechanism in hereditary spastic paraplegia type SPG8. *Orphanet Journal of Rare Diseases*, **10**: 147.

Jamra RA, Philippe O, Raas-Rothschild A, et al. 2011. Adaptor protein complex 4 deficiency causes severe autosomal-recessive intellectual disability, progressive spastic paraplegia, shy character, and short stature. *The American Journal of Human Genetics*, **88**(6): 788−795.

Kaepernick L, Legius E, Higgins J, et al. 1994. Clinical aspects of the MASA syndrome in a large family, including expressing females. *Clinical Genetics*, **45**(4): 181−185.

Karczewski KJ, Francioli LC, Tiao G, et al. 2020. The mutational constraint spectrum quantified from variation in 141, 456 humans. *Nature*, **581**(7809): 434−443.

Klebe S, Stevanin G, Depienne C. 2015. Clinical and genetic heterogeneity in hereditary spastic paraplegias: from SPG1 to SPG72 and still counting. *Revue Neurologique*, **171**(6–7): 505–530.

Komachali SR, Sheikholeslami M, Salehi M. 2022. A novel mutation in *GJC2* associated with hypomyelinating leukodystrophy type 2 disorder. *Genomics & Informatics*, **20**(2): e24.

Kruer MC, Paudel R, Wagoner W, et al. 2012. Analysis of *ATP13A2* in large neurodegeneration with brain iron accumulation (NBIA) and dystonia-parkinsonism cohorts. *Neuroscience Letters*, **523**(1): 35−38.

Lemon RN. 2008. Descending pathways in motor control. *Annual Review of Neuroscience*, **31**: 195−218.

Li ML, Wu SH, Zhang JJ, et al. 2019. 547 transcriptomes from 44 brain areas reveal features of the aging brain in non-human primates. *Genome Biology*, **20**(1): 258.

Liu WT, Venugopal S, Majid S, et al. 2020. Single-cell RNA-seq analysis of the brainstem of mutant SOD1 mice reveals perturbed cell types and pathways of amyotrophic lateral sclerosis. *Neurobiology of Disease*, **141**: 104877.

Loomba S, Straehle J, Gangadharan V, et al. 2022. Connectomic comparison of mouse and human cortex. *Science*, **377**(6602): eabo0924.

Lossos A, Elazar N, Lerer I, et al. 2015. Myelin-associated glycoprotein gene mutation causes Pelizaeus-Merzbacher disease-like disorder. *Brain*, **138**(Pt 9): 2521–2536.

MacLean M, López-Díez R, Vasquez C, et al. 2022. Neuronal-glial communication perturbations in murine *SOD1*^{G93A} spinal cord. *Communications Biology*, **5**(1): 177.

Mannan AU, Krawen P, Sauter SM, et al. 2006. ZFYVE27 (SPG33), a novel spastin-binding protein, is mutated in hereditary spastic paraplegia. *The American Journal of Human Genetics*, **79**(2): 351−357.

Mao F, Li ZH, Zhao BY, et al. 2015. Identification and functional analysis of a SLC33A1: c. 339T>G (p. Ser113Arg) variant in the original SPG42 family. *Human Mutation*, **36**(2): 240−249.

Matsumoto N, Watanabe N, Iibe N, et al. 2019. Hypomyelinating leukodystrophy-associated mutation of RARS leads it to the lysosome, inhibiting oligodendroglial morphological differentiation. *Biochemistry and Biophysics Reports*, **20**: 100705.

Meijer IA, Dion P, Laurent S, et al. 2007. Characterization of a novel SPG3A deletion in a French-Canadian family. *Annals of Neurology*, **61**(6): 599−603.

Mifflin L, Hu ZR, Dufort C, et al. 2021. A RIPK1-regulated inflammatory microglial state in amyotrophic lateral sclerosis. *Proceedings of the National Academy of Sciences of the United States of America*, **118**(13): e2025102118.

Montecchiani C, Pedace L, Lo Giudice T, et al. 2016. ALS5/SPG11/*KIAA1840* mutations cause autosomal recessive axonal Charcot-Marie-Tooth disease. *Brain*, **139**(Pt 1): 73–85.

Montenegro G, Rebelo AP, Connell J, et al. 2012. Mutations in the ER-shaping protein reticulon 2 cause the axon-degenerative disorder hereditary spastic paraplegia type 12. *The Journal of Clinical Investigation*, **122**(2): 538−544.

Muglia M, Magariello A, Nicoletti G, et al. 2002. Further evidence that *SPG3A* gene mutations cause autosomal dominant hereditary spastic paraplegia. *Annals of Neurology*, **51**(6): 794−795.

Namboori SC, Thomas P, Ames R, et al. 2021. Single-cell transcriptomics identifies master regulators of neurodegeneration in SOD1 ALS iPSC-derived motor neurons. *Stem Cell Reports*, **16**(12): 3020−3035.

Neuser S, Brechmann B, Heimer G, et al. 2021. Clinical, neuroimaging, and molecular spectrum of *TECPR2*-associated hereditary sensory and autonomic neuropathy with intellectual disability. *Human Mutation*, **42**(6): 762−776.

Online Mendelian Inheritance in Man. 2021. OMIM Phenotypic Series - PS303350. in Spastic paraplegia - PS303350. Vol. 2021. McKusick-Nathans Institute of Genetic Medicine, Johns Hopkins University (Baltimore, MD).

Orphanet Rare Disease Portal. 2021. Orphanet rare disease portal. Vol. 2021.

Orso G, Martinuzzi A, Rossetto MG, et al. 2005. Disease-related phenotypes in a *Drosophila* model of hereditary spastic paraplegia are ameliorated by treatment with vinblastine. *Journal of Clinical Investigation*, **115**(11): 3026−3034.

Orthmann-Murphy JL, Salsano E, Abrams CK, et al. 2009. Hereditary spastic paraplegia is a novel phenotype for *GJA12*/*GJC2* mutations. *Brain*, **132**(Pt 2): 426–438.

Orvis J, Gottfried B, Kancherla J, et al. 2021. gEAR: Gene Expression Analysis Resource portal for community-driven, multi-omic data exploration. *Nature Methods*, **18**(8): 843−844.

Panza E, Escamilla-Honrubia JM, Marco-Marín C, et al. 2016. *ALDH18A1* gene mutations cause dominant spastic paraplegia SPG9: loss of function effect and plausibility of a dominant negative mechanism. *Brain*, **139**(Pt 1): e3.

Pujol C, Legrand A, Parodi L, et al. 2021. Implication of folate deficiency in CYP2U1 loss of function. *Journal of Experimental Medicine*, **218**(11): e20210846.

Robinson MD, Oshlack A. 2010. A scaling normalization method for differential expression analysis of RNA-seq data. *Genome Biology*, **11**(3): R25.

Ruano L, Melo C, Silva MC, et al. 2014. The global epidemiology of hereditary ataxia and spastic paraplegia: a systematic review of prevalence studies. *Neuroepidemiology*, **42**(3): 174−183.

Saez-Atienzar S, Bandres-Ciga S, Langston RG, et al. 2021. Genetic analysis of amyotrophic lateral sclerosis identifies contributing pathways and cell types. *Science Advances*, **7**(3): eabd9036.

Scala F, Kobak D, Bernabucci M, et al. 2021. Phenotypic variation of transcriptomic cell types in mouse motor cortex. *Nature*, **598**(7879): 144−150.

Ségalat L. 2007. Loss-of-function genetic diseases and the concept of pharmaceutical targets. *Orphanet Journal of Rare Diseases*, **2**: 30.

Song L, Rijal R, Karow M, et al. 2018. Expression of N471D strumpellin leads to defects in the endolysosomal system. *Disease Models & Mechanisms*, **11**(9): dmm033449.

Szebényi K, Wenger LMD, Sun Y, et al. 2021. Human ALS/FTD brain organoid slice cultures display distinct early astrocyte and targetable neuronal pathology. *Nature Neuroscience*, **24**(11): 1542−1554.

Tesson C, Nawara M, Salih MAM, et al. 2012. Alteration of fatty-acid-metabolizing enzymes affects mitochondrial form and function in hereditary spastic paraplegia. *The American Journal of Human Genetics*, **91**(6): 1051−1064.

Tsai PC, Huang YH, Guo YC, et al. 2014. A novel *TFG* mutation causes

Charcot-Marie-Tooth disease type 2 and impairs TFG function. *Neurology*, **83**(10): 903−912.

Tüysüz B, Bilguvar K, Koçer N, et al. 2014. Autosomal recessive spastic tetraplegia caused by *AP4M1* and AP4B1 gene mutation: expansion of the facial and neuroimaging features. *American Journal of Medical Genetics Part A*, **164**(7): 1677−1685.

Uhlen M, Fagerberg L, Hallström BM, et al. 2015. Tissue-based map of the human proteome. *Science*, **347**(6220): e1260419.

Van Den Berg RA, Hoefsloot HCJ, Westerhuis JA, et al. 2006. Centering, scaling, and transformations: improving the biological information content of metabolomics data. *BMC Genomics*, **7**: 142.

Vandamme TF. 2014. Use of rodents as models of human diseases. *Journal of Pharmacy & BioAllied Sciences*, **6**(1): 2−9.

Vaz FM, McDermott JH, Alders M, et al. 2019. Mutations in *PCYT2* disrupt etherlipid biosynthesis and cause a complex hereditary spastic paraplegia. *Brain*, **142**(11): 3382−3397.

Veitia RA, Caburet S, Birchler JA. 2018. Mechanisms of Mendelian dominance. *Clinical Genetics*, **93**(3): 419−428.

Walusinski O. 2020. A historical approach to hereditary spastic paraplegia. *Revue Neurologique*, **176**(4): 225−234.

Winter RM, Davies KE, Bell MV, et al. 1989. MASA syndrome: further clinical delineation and chromosomal localisation. *Human Genetics*, **82**(4): 367−370.

Xu M, Zhang DF, Luo RC, et al. 2018. A systematic integrated analysis of brain expression profiles reveals *YAP1* and other prioritized hub genes as important upstream regulators in Alzheimer's disease. *Alzheimer's & Dementia*, **14**(2): 215−229.

Yao ZZ, Van Velthoven CTJ, Nguyen TN, et al. 2021. A taxonomy of transcriptomic cell types across the isocortex and hippocampal formation. *Cell*, **184**(12): 3222−3241.e26.

Yıldırım Y, Orhan EK, Iseri SAU, et al. 2011. A frameshift mutation of *ERLIN2* in recessive intellectual disability, motor dysfunction and multiple joint contractures. *Human Molecular Genetics*, **20**(10): 1886−1892.

Yim AKY, Wang PL, Bermingham JR et al. 2022. Disentangling glial diversity in peripheral nerves at single-nuclei resolution. *Nature Neuroscience*, **25**(2): 238−251.